Bioconjugate Chemistry

Article

pubs.acs.org/bc

In Vitro and *In Vivo* Analysis of Indocyanine Green-Labeled Panitumumab for Optical Imaging—A Cautionary Tale

Yang Zhou, Young-Seung Kim, Diane E. Milenic, Kwamena E. Baidoo, and Martin W. Brechbiel*

Radioimmune & Inorganic Chemistry Section, Radiation Oncology Branch, National Cancer Institute, 10 Center Drive, Bethesda, Maryland 20892, United States

Supporting Information

ABSTRACT: Indocyanine green (IC-Green), the only FDA approved near-infrared (NIR) fluorophore for clinical use, is attractive to researchers for the development of targeted optical imaging agents by modification of its structure and conjugation to monoclonal antibodies (mAbs) or their fragments. IC-Green derivative, ICG-sulfo-OSu (ICG-sOSu), is frequently used for antibody conjugation. However, ICG-sOSu is amphiphilic and readily facilitates aggregation of mAbs that is not easily separable from the desired immunoconjugates. Complications originating from this behavior are frequently overlooked by researchers. This study examined detailed chemical and biological characteristics of an ICG-sOSu-labeled mAb, panitumumab, and provided a clinically applicable strategy to deliver a pure conjugation product. Size-exclusion high-performance liquid chromatography (SE-HPLC) analysis of conjugation reactions, performed at molar reaction ratios of ICG-sOSu: mAb of 5, 10, or 20, resulted in isolable desired ICG-sOSu-panitumumab conjugation product in 72%, 53%, and 19% yields, respectively, with the remainder consisting of high molecular weight aggregates (>150 kDa) 14%, 30%, and 51%, respectively. The HPLC-purified ICG-sOSu-panitumumab products were analyzed by native and SDS polyacrylamide gel electrophoresis (PAGE) followed by optical imaging. Results indicated that the interaction between ICG-sOSu and panitumumab was due to both covalent and noncovalent binding of the ICG-sOSu to the protein. Noncovalently bound dye in the ICG-sOSu-panitumumab conjugate products was removed by extraction with ethyl acetate to further purify the HPLC-isolated conjugation products. With conserved immunoreactivity, excellent target-specific uptake of the doubly purified bioconjugates was observed with minimal liver retention in athymic nude mice bearing HER1-expressing tumor xenografts. In summary, the preparation of well-defined bioconjugate products labeled with commercial ICG-sOSu dye is not a simple process and control of the conjugation reaction ratio and conditions is crucial. Furthermore, absolute purification and characterization of the products is necessitated prior to *in vivo* optical imaging. Use of validated and characterized dye conjugate products should facilitate the development of clinically viable and reproducible IC-Green derivative and other NIR dye mAb conjugates for optical imaging applications.

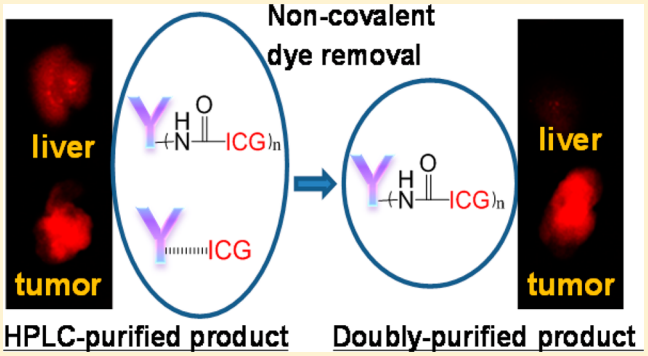

INTRODUCTION

In recent years optical molecular imaging technology has gained remarkable attention for cancer visualization, characterization, and localization. Optical imaging is not only a real-time modality that is nonionizing and highly sensitive; it is also cost-effective with considerable ease in preparation of molecular imaging agents. Its potential application for use in image-guided surgery has also been successfully demonstrated.[1−3] Due to significant attenuation of the visible light spectrum in tissues, near-infrared fluorescence (NIRF) is frequently used in optical imaging and can detect signals as deep as 7−14 cm.[4] Indocyanine green (IC-Green) is the only NIRF dye approved for clinical use, most commonly for medical diagnosis, with a penetration depth of 0.55−5 cm depending on the tissue properties.[5,6] The specificity of IC-Green depends highly on application, e.g., intravenous injection for angiography or local injection for sentinel node identification. Although it has been used for real-time fluorescence imaging to guide surgical resection of tumor,[7,8] it is not specific to cancer targets and as such may generate false positive results.[9] This dye is attractive to researchers for the development of targeted optical imaging agents upon modification and conjugation to antibodies (Abs) or their fragments.[10−14] Target-specific IC-Green bioconjugates are expected to result in more accurate and reliable results. For example, linking with an Ab after assembly with phospholipid-polyethylene glycol (PL−PEG) to form a nanostructure has successfully demonstrated the potential for targeted optical imaging and photothermal therapy in cancer cells.[15] These studies provide significant encouragement for future applica-

Received: July 16, 2014
Revised: September 8, 2014
Published: September 22, 2014

tions of IC-Green and its derivative-conjugated Abs for targeted optical imaging of cancer.

IC-Green, however, is an amphiphilic molecule capable of self-organization to form highly ordered aggregates via van der Waals forces and hydrophobic interactions.[16] Although this behavior has been noted to be dependent on dye concentration, solvent, ionic strength, pH, and temperature, the size profile of the aggregates has not been analyzed by size-exclusion HPLC (SE-HPLC) or other modalities.[17] Importantly, this behavior contributes to the formation of high molecular weight (HMW) aggregates (>150 kDa) during protein conjugation reactions[18] that are not reasonably removed by dialysis or PD-10 filtration. This problem seems to be frequently overlooked by researchers.[10−13] As a result IC-Green-related conjugation products in previously published reports appear not to have been well examined for these complications potentially compromising prior reported results. If the undesired aggregates are not removed, they may lead to significant changes in the optical properties of the desired conjugate products,[16] as well as impact an accurate measurement of the amount of dye conjugated to protein, and other characterization criteria, and compromise *in vivo* applications.

Previous studies from this laboratory demonstrated specific, high efficiency targeting of panitumumab in HER1-positive tumors in multiple xenograft models.[19,20] ICG-*N*-hydroxysulfosuccinimide ester (abbreviated as ICG-sOSu here) (Scheme 1), commonly used in literature publications for antibody conjugation, was employed in this study because it provides an established starting material amenable to aqueous conjugation reactions.[10−13] In fact, this project began with the intent of generating ICG-sOSu-panitumumab to serve as a reference and control for subsequent studies. To characterize and purify ICG-sOSu-panitumumab conjugates, SE-HPLC was used to define conjugation reaction conditions that might provide a balance between high quality functional conjugation product(s) versus aggregation products. This was prompted by initial observations of the formation of HMW aggregates (>150 kDa) by SE-HPLC.[18] The conjugation reaction products were examined further by SDS and native PAGE. In this study, evidence of significant amounts of noncovalently bound ICG-sOSu in the SE-HPLC-purified conjugation products was observed, a result not addressed in prior literature, and the abrogation of this complication is reported. Herein, the characterization and validation of purified ICG-sOSu-panitumumab conjugates suitable for imaging HER1-positive tumors is reported.

Scheme 1. Schematic Conjugation of mAb Panitumumab to ICG-sulfo-OSu at Dye:Protein Molar Ratios of 5, 10, or 20[a]

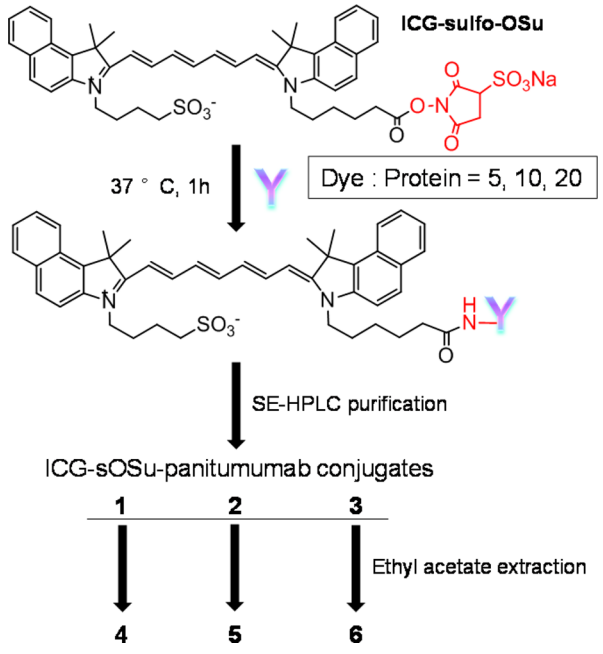

[a]SE-HPLC was first applied to purify conjugation products and yield products **1**, **2**, and **3**, respectively. Thereafter, the SE-HPLC purified products were extracted with ethyl acetate to yield products **4**, **5**, and **6**, respectively.

RESULTS

Preparation and Characterization of ICG-sOSu-Panitumumab Conjugates. Panitumumab was reacted with the amine-reactive ICG-sOSu at dye: mAb molar ratios of 5, 10, or 20 (5×, 10×, or 20×) to yield three ICG-sOSu-panitumumab conjugates, **1**, **2**, and **3**, respectively (Scheme 1). After the reaction, the three conjugate solutions were first analyzed and then purified by SE-HPLC. In all cases, undesired HMW aggregates (>150 kDa) were observed with retention times (RTs) of 11.5−18 min (Figure 1). Noticeably, as higher amounts of ICG-sOSu were reacted with panitumumab, correspondingly greater amounts of aggregates (∼14%, 30%, and 51% for 5×, 10×, and 20×, respectively) (Table 1) were generated. The percentages of isolable ICG-sOSu-panitumumab conjugates (**1**, **2**, **3**) produced correspondingly decreased and were ∼52%, 28%, and 9% for 5×, 10×, and 20×, respectively, as determined by SE-HPLC. In addition, the peak at 12.5 min dramatically increased with increased ratios of ICG-sOSu in the conjugation reaction. Collection and inspection of the late peak at 27.2 min revealed that no ICG-sOSu dye was present as measured by spectrophotometer from 600 to 900 nm, in contrast to the visible green color in the samples collected for the peaks corresponding to either aggregate or desired conjugate. This lack of absorbance suggests all excess ICG-sOSu in the reaction to be associated with either the aggregate species or desired conjugation product, with this late peak primarily composed of impurities originating from the commercial ICG-sOSu (Supporting Information Figure S1). If this low molecular weight species (LMW) is excluded from the data analysis, when the SE-HPLC profiles are reintegrated, the purified ICG-sOSu-panitumumab conjugates represent 61%, 36%, and 17% for 5×, 10×, and 20×, respectively. Initially, the desired ICG-sOSu-panitumumab conjugates were each purified by SE-HPLC, resulting in a final purity of >99% (Figure 1). As a control reference, a CD33-specific antibody HuM195 was also conjugated with ICG-sOSu at an ICG-sOSu: mAb molar ratio of 10 (10×). Aggregate species were also observed and subsequently removed by SE-HPLC (Table 1, Supporting Information Figure S2).

All three HPLC-purified ICG-sOSu-panitumumab conjugates (**1**, **2**, and **3**) exhibited two absorbance peaks at 720 and 800 nm; the intensity ratio between the two absorbance peaks, 720 nm relative to 800 nm, increased with increasing equivalents of ICG-sOSu (Figure 2A). The average number of ICG-sOSu conjugated to panitumumab was determined to be ∼1, 2, and 5 for **1**, **2**, and **3**, respectively, while that of ICG-sOSu-HuM195 was calculated to be ∼1 (Table 1). Additionally, molecular weights of the HMW aggregates were calculated

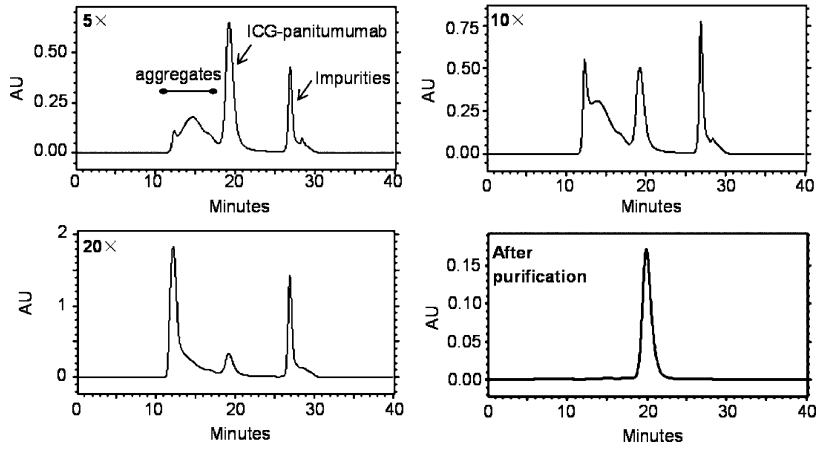

Figure 1. SE-HPLC profiles of conjugation reaction mixtures (5×, 10×, and 20×) and the representative purified bioconjugate. High molecular weight aggregates were observed with retention times at 11.5−18 min. Molecular weight standards: 670 kDa (14.3 min), 158 kDa (19.2 min), and 1.35 kDa (27.1 min).

Table 1. Summary Data of ICG-sOSu-Panitumumab (5×, 10×, and 20× Reaction) and ICG-sOSu-HuM195 (10× Reaction) Bioconjugates

reaction	retention time	aggregates% (before purification)	conjugates% (before purification)	conjugates% (after purification)	yield (%)	# of ICG-sOSu conjugated to panitumumab
			ICG-sOSu-panitumumab			
5×	19.2 min	14	52	99	72	1
10×	19.2 min	30	28	99	53	2
20×	19.2 min	51	9	99	19	5
			ICG-sOSu-HuM195			
10×	18.6 min	17	45	99	80	1

from the linear plot of protein standards with the highest being ≥2000 kDa. Because the peak (RT = 12.5 min) was large and comprised significant amounts of mAb in the reaction with 20× ICG-sOSu dye, the percent yield of the desired ICG-sOSu-panitumumab product in this reaction was low (~19%). Positively, the competition assay demonstrated that the immunoreactivity was retained for all three of the HPLC-isolated ICG-sOSu-panitumumab conjugates for HER-1, with IC_{50} values of 0.67 ± 0.07 nM, 0.82 ± 0.08 nM, and 0.53 ± 0.13 nM, for **1**, **2**, and **3**, respectively, compared with the IC_{50} value of 0.67 ± 0.07 nM for intact native panitumumab (Figure 2B).

***In Vitro* and *In Vivo* Studies of SE-HPLC-Isolated ICG-sOSu-Panitumumab.** The potential for optical imaging was examined for all three SE-HPLC-purified ICG-sOSu-panitumumab conjugates (**1**, **2**, and **3**) *in vitro* using HER1-expressing human epidermoid carcinoma A431 cancer cells. ICG-sOSu-panitumumab (**3**) possessed the highest fluorescence intensity staining of A431 cells (Supporting Information Figure S3), followed by **2** and **1**. In contrast, no fluorescence signal was obtained with the A431 cells after incubation with ICG-sOSu-HuM195.

For *in vivo* imaging studies, ICG-sOSu-panitumumab conjugates (**1** and **2**) were administered to athymic nude mice bearing HER1-positive s.c. LS-174T xenografts. Due to the low product yield from the 20× reaction with ICG-sOSu, conjugate **3** was not carried forward. Tumors were clearly visualized 24 h after intravenous injection of ICG-sOSu-panitumumab conjugate (**2**, 20 μg) through day 7, during which the background fluorescence gradually diminished (Figure 3A). Upon excision of tissue at day 3 postinjection of the conjugation products, the tumor showed the highest fluorescence signal followed by the liver with the second highest intensity (Figure 3B). To demonstrate the specificity of the bioconjugates, excess panitumumab injected 1 h prior to administration of ICG-sOSu-panitumumab successfully blocked tumor uptake (Figure 3C). No localization to tumor (Figure 3C) was observed in the mice injected with the CD33-specific ICG-sOSu-HuM195 control, further demonstrating the specificity of ICG-sOSu-panitumumab. Quantitative analysis indicated a superior tumor-to-background ratio with product **2** over that of **1** at days 3 and 7 with doses of 10 μg and 20 μg ($p < 0.01$); however, there was no significant difference at days 1 and 2 ($p > 0.05$) (Figure 3D). *Ex vivo* imaging studies were also performed in mice bearing HER1-positive peritoneal LS-174T tumor xenografts. Similar to the previous study, the highest fluorescence intensity was obtained in the tumor followed by the liver (Supporting Information Figure S4).

ICG-sOSu Covalently and Noncovalently Bound to Panitumumab. Because it is well-known that IC-Green may bind to proteins via noncovalent interaction,[3,21] it would be important to determine whether ICG-sOSu bound to panitumumab covalently or noncovalently. The SE-HPLC-purified ICG-sOSu-panitumumab was also evaluated by SDS-PAGE and visualized using Colloidal Blue stain for protein staining and optical imaging to detect the presence of ICG-sOSu. Under nonreducing conditions, protein staining of the three conjugated products (**1**, **2**, and **3**) exhibited bands similar to the unmodified panitumumab (Figure 4A). Two distinct bands were evident at ~170 and 200 kDa which increased in intensity corresponding with the increasing ICG-sOSu used in the reaction. These bands were the predominant components in the collected fractions corresponding to the HMW species noted in the SE-HPLC profile. The molecular weights of the

dx.doi.org/10.1021/bc500312w | *Bioconjugate Chem.* 2014, 25, 1801−1810

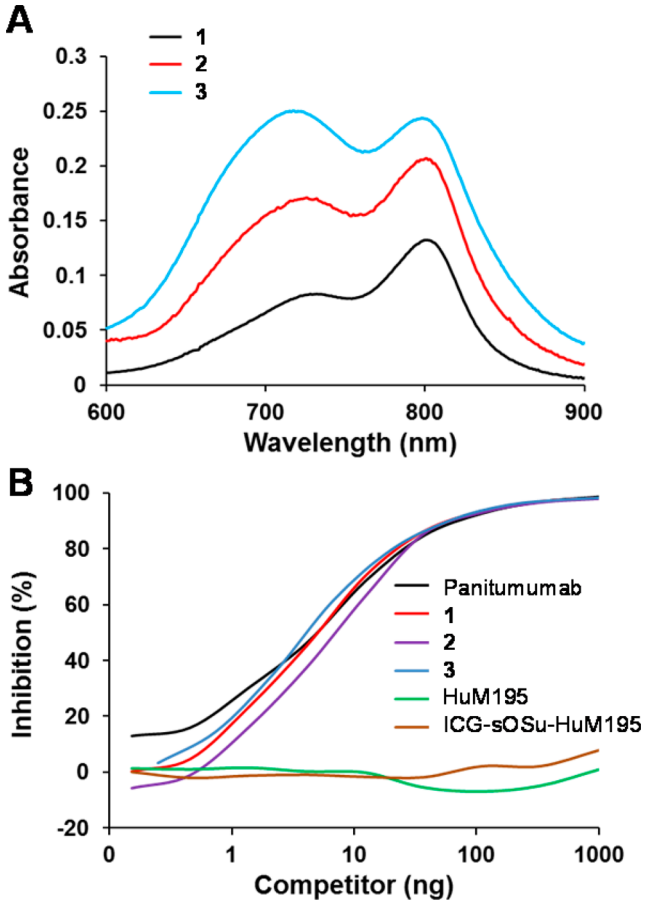

Figure 2. (A) Absorption spectra of SE-HPLC-purified ICG-sOSu-panitumumab (**1**, **2**, and **3**) from 600 to 900 nm. (B) Competition radioimmunoassay of SE-HPLC-purified ICG-sOSu-panitumumab (**1**, **2**, and **3**) with ^{125}I-panitumumab. ICG-sOSu-HuM195 and HuM195 served as negative controls while unmodified panitumumab served as a positive control.

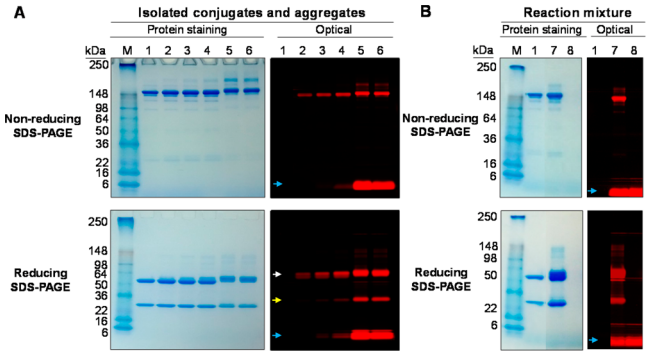

Figure 4. SDS-PAGE of (A) SE-HPLC-isolated ICG-sOSu-panitumumab conjugates and aggregates, and (B) reaction mixture, under nonreducing and reducing conditions with β-mercaptoethanol. Panitumumab served as a reference. Colloidal blue protein staining and optical imaging were performed: M, marker; 1, intact panitumumab antibody; 2, **1**; 3, **2**; 4, **3**; 5, ICG-sOSu aggregates (from 20× reaction, peak with RT = 12.5 min); 6, ICG-sOSu aggregates (from 20× reaction, peak with RT = 14.5 min); 7, ICG-sOSu-panitumumab reaction mixture (10×, without purification); 8, ICG-sOSu alone incubated in conjugation buffer for 1 h at 37 °C as a control. White arrow: heavy chain; yellow arrow: light chain; blue arrow: free dye.

components were significantly lower than that seen by SE-HPLC (MW ≥ 2000 kDa), suggesting that the noncovalent bonds in the aggregates were disrupted by SDS. The number of ICG-sOSu molecules covalently linked to aggregated panitumumab in the lower and upper band species was determined to be ~30−50 calculated from the linear plot of log MW of protein markers vs relative migration distance; however, the majority of the ICG-sOSu in the aggregates was noncovalently associated as evidenced by the corresponding optically active LMW entity on the gel (blue arrow, Figure 4A). This LMW band is also present, with increasing intensity, in the three preparations of the ICG-sOSu-panitumumab conjugate. This result highlights some of the differences between running a

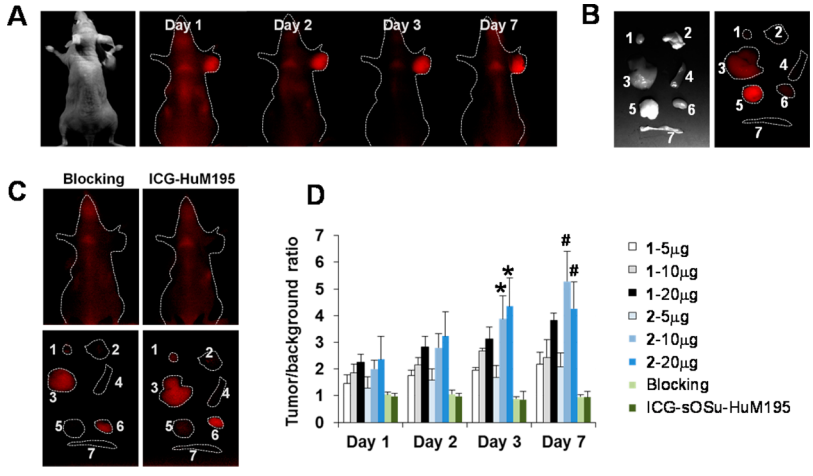

Figure 3. (A) Representative *in vivo* NIR fluorescence imaging of athymic mice bearing HER1-positive s.c. LS-174T xenografts at days 1, 2, 3, and 7 after i.v. injection of SE-HPLC-purified ICG-sOSu-panitumumab (**2**, 20 μg). (B) Representative *ex vivo* NIR fluorescence image (right) of the dissected organs at day 3. Labels: 1, heart; 2, lung; 3, liver; 4, spleen; 5, tumor; 6, kidney; 7, intestine. Note: The white light image in (B) indicates the order of the organs shown in (B) and (C). (C) Representative *in vivo* and *ex vivo* fluorescence images of HER1-positive s.c. LS-174T tumor-bearing mice with excess antibody blocking or with ICG-sOSu-HuM195 (negative control). (D) Comparison of tumor-to-background ratio with injection of various doses of SE-HPLC-purified ICG-sOSu-panitumumab (**1**, **2**) in athymic mice bearing HER1-positive s.c. LS-174T xenografts (n = 5). *, significantly different from **2** - 5 μg group (day 3) (P < 0.001); #, significantly different from **2** - 5 μg group (day 7) (P < 0.01).

dx.doi.org/10.1021/bc500312w | *Bioconjugate Chem.* 2014, 25, 1801−1810

native versus an SDS modified gel assay. In the absence of SDS, the protein stained gel reveals HMW aggregates were mostly retained at the well of the stacking gel (Figure 5A); interestingly, broad smearing of the HMW aggregates is apparent when visualized by the NIRF.

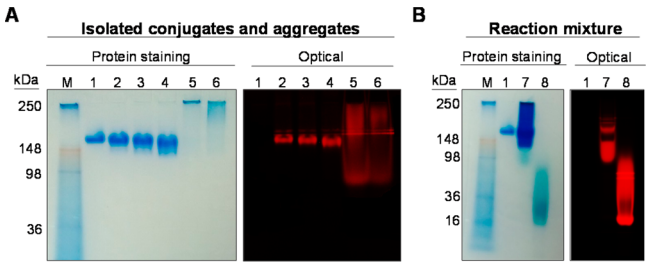

Figure 5. Native gel of (A) SE-HPLC-isolated ICG-sOSu-panitumumab conjugates and aggregates, and (B) reaction mixture. Panitumumab served as a reference. Colloidal blue protein staining and optical imaging were performed: M, marker; 1, intact panitumumab antibody; 2, **1**; 3, **2**; 4, **3**; 5, ICG-sOSu aggregates (from 20× reaction, peak with RT = 12.5 min); 6, ICG-sOSu aggregates (from 20× reaction, peak with RT = 14.5 min); 7, ICG-sOSu-panitumumab reaction mixture (10×, without purification); 8, ICG-sOSu alone incubated in conjugation buffer for 1 h at 37 °C as a control.

Although the above-mentioned data suggest that the mAb panitumumab was a component of the HMW aggregates, it is equally important to establish whether ICG-sOSu itself can also form HMW aggregates. To address this point, SDS- and native PAGE were performed using samples of ICG-sOSu-panitumumab reaction mixture (without purification) and ICG-sOSu alone after incubation in conjugation buffer for 1 h at 37 °C. Optical imaging of the gel indicated that the reaction mixture (Figure 5B) contains a distinct band at ~150 kD, consistent with the expected molecular weight of panitumumab. There is also a broad band from 64 to 98 kDa. This broad band appears as a single band in the presence of SDS (Figure 4B) as determined by optical imaging. The colloidal blue staining for protein, meanwhile, indicated a range of molecular weights from 98 kDa to 250 kDa. These HMW entities are also evidenced by a broad band of fluorescence, while the SDS-PAGE showed one fluorescent LMW band for the ICG-sOSu sample (blue arrow, Figure 4B), whereas the sample from the ICG-sOSu-panitumumab conjugation reaction mixture showed multiple HMW entities under nonreducing conditions (Figure 4B).

Under reducing conditions, the pattern of protein bands was again similar for the bioconjugates (**1**, **2**, and **3**) compared to unmodified panitumumab (Figure 4A). HMW species were present, seen as a smear of staining above the heavy chain ranging in M_r from ~64 to 100. The staining intensity increases with the increasing amount of dye used in the reaction. These same patterns are evident when developed for the NIRF. The majority of the ICG-sOSu appears to be linked to the heavy chain (>80%) as illustrated by the optical imaging in Figure 4A (white arrow). The LMW species was also evident under optical imaging in the SE-HPLC-purified conjugation products, particularly so in product **3**. The presence of this LMW band suggests two scenarios: (1) there is either unreacted or hydrolyzed ICG-sOSu dye, or (2) there is ICG-sOSu noncovalently bound to the panitumumab. To examine these possibilities, a peak portion of the conjugation products was collected by SE-HPLC with the retention time 19–20 min, in contrast to 18.5–20.5 min (Figure 1). Results showed that the LMW species were retained (Figure 6A), thus excluding the

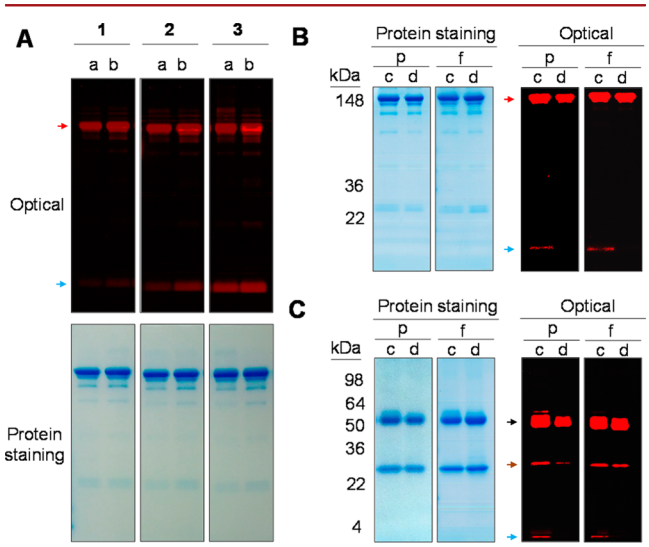

Figure 6. (A) SDS-PAGE of the SE-HPLC-isolated ICG-sOSu-panitumumab (**1**, **2**, and **3**). a: samples collected from SE-HPLC RT 18.5 to 20.5 min. b: samples collected from HPLC RT 19–20 min. (B–C) SDS-PAGE of SE-HPLC-isolated ICG-sOSu-panitumumab before (c, **2**) and after (d, **5**) extraction by ethyl acetate under (B) nonreducing and (C) reducing condition. Samples were loaded with the same protein level (p) or equal amount of fluorophore (f). Colloidal blue protein staining and optical imaging were performed after development. Black arrow, heavy chain; brown arrow, light chain; blue arrow, free dye; red arrow, desired conjugation product.

possibility of unreacted or hydrolyzed ICG-sOSu dye. Optical imaging of the native gel showed only one band for all the SE-HPLC-purified bioconjugates further confirming the origin of the LMW bands to be noncovalently associated ICG-sOSu dissociated by the SDS (Figure 5A). To further investigate this observation, ethyl acetate[22] was used to extract the non-covalently bound ICG-sOSu from the ICG-sOSu-panitumumab conjugates (**1**, **2**, and **3**), and produce three new products, **4**, **5**, and **6**, respectively. As seen from SDS-PAGE of the extracted conjugate, the LMW entity appears to be totally eliminated by this step (Figure 6B–C). The percentages of the covalent interaction in these conjugated products were calculated to be ~75%, 61%, and 46% for the thus treated **1**, **2**, and **3**, respectively (Figure 7A).

***In Vitro* and *In Vivo* Characterization of Doubly Purified ICG-sOSu-Panitumumab.** To determine if the doubly purified ICG-sOSu-panitumumab, by both SE-HPLC and ethyl acetate extraction (see Supporting Information Figure S5 for SE-HPLC of the doubly purified conjugate), retained its potential for optical imaging, product **2** was selected. A competition radioimmunoassay was performed to demonstrate that the immunoreactivity against HER-1 was conserved in the ICG-sOSu-panitumumab even after extraction with ethyl acetate (Figure 7B). For the animal study, doses administered to athymic nude mice bearing HER1-positive s.c. LS-174T xenografts were normalized to match the amounts in the initial imaging study by either equal protein (20 μg) or same amount of fluorophore because the amount of ICG-sOSu conjugated to panitumumab was reduced to 1.2 from 2.1 after ethyl acetate extraction. Optical imaging was carried out up to 7 days

dx.doi.org/10.1021/bc500312w | *Bioconjugate Chem.* 2014, 25, 1801–1810

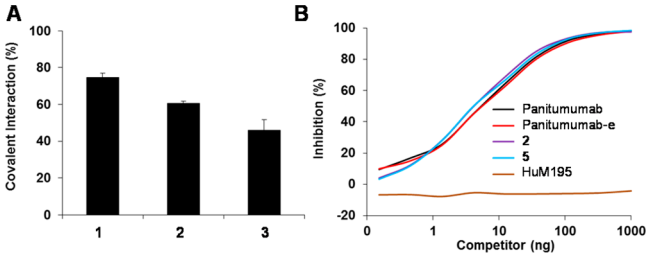

Figure 7. (A) Percentages of covalent interaction in the SE-HPLC-isolated ICG-sOSu-panitumumab conjugates (**1**, **2**, **3**). Ethyl acetate was used to remove noncovalently bound ICG-sOSu. (B) Competition radioimmunoassay, with ^{125}I-panitumumab, of SE-HPLC-isolated ICG-sOSu-panitumumab before (**2**) and after (**5**) extraction by ethyl acetate. Unmodified panitumumab monoclonal antibody served as a positive control. In addition, unmodified panitumumab after ethyl acetate extraction (panitumumab-e) was also examined. HuM195 served as a negative control.

postinjection of the new product **5**. With equivalent dye, comparable tumor-to-background ratios were observed for the SE-HPLC-isolated products prior to and post extraction with ethyl acetate (Figure 8A). When compared on the basis of equivalent protein, the tumor-to-background ratio of the doubly purified **5** seemed to be lower as compared with that of the bioconjugate prior to extraction, but this difference was not significant ($p > 0.05$) (Figure 8A). However, and importantly, there was an improvement in the liver clearance, with significantly reduced fluorescence intensity noted ($p < 0.01$) (Figure 8B). The tumor-to-liver ratio was significantly increased after ethyl acetate extraction confirming advantages of using the doubly purified conjugation product (Figure 8C).

DISCUSSION

This report, for the first time, provides a detailed description of the full purification, characterization, and validation of an ICG-sOSu-conjugated mAb, and proposes a clinically applicable strategy to produce and purify covalently bound dye conjugation products. Analysis of the conjugation reaction between ICG-sOSu dye and a mAb (panitumumab) revealed that there is formation of a considerable amount of HMW aggregates (>150 kDa) in the reaction mixtures that are apparently overlooked in the literature.[10−13] The amounts of aggregation product are clearly directly influenced by the amounts of dye in the reaction, which also decreases the amounts of isolable conjugation products. However, these aggregates could clearly be removed by SE-HPLC or other size-exclusion separation methodologies. More importantly, the interaction between ICG-sOSu and panitumumab in the SE-HPLC isolated conjugation reaction product was found to be both covalent and noncovalent in nature and would posit that the use of other size-exclusion separation methodologies would provide the same conclusion. Accordingly, a further purification step was performed, namely, ethyl acetate extraction, to abrogate noncovalently bound ICG-sOSu. This step was in fact reported in one of the earlier publications regarding the development of bifunctional ICG-sOSu that also provided an impetus for a closer investigation of possible noncovalent interactions that should have been noted by others seeking to use ICG-sOSu-mAb conjugates for imaging.[22] Importantly, the doubly purified bioconjugate exhibited conservation of immunoreactivity contrary to the generally held conventional wisdom that this step would simply denature the protein or

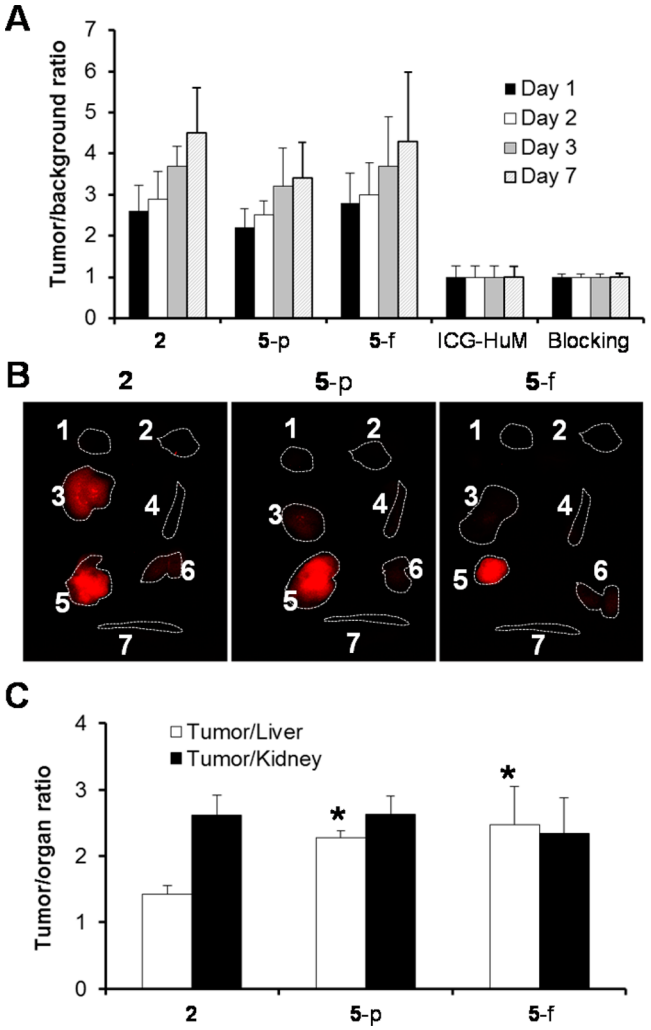

Figure 8. (A) Comparison of tumor-to-background ratio with injection of SE-HPLC isolated **2** and after extraction by ethyl acetate **5** in athymic mice bearing HER1-positive s.c. LS-174T xenografts (n = 5). The dose of **5** was administered after normalization by the same protein (**5**-p, 20 mg) or fluorophore (**5**-f). (B) Representative *ex vivo* NIR fluorescence image of the dissected organs from mice above at day 3 after i.v. injection of doses. Labels: 1, heart; 2, lung; 3, liver; 4, spleen; 5, tumor; 6, kidney; 7, intestine. (C) Tumor-to-liver and tumor-to-kidney ratios obtained from the *ex vivo* imaging. *, significantly different from product **2** ($P < 0.01$).

compromise the structure of the mAb eliminating any possibility of reacting with the cognate antigen, HER1. *In vivo* re-evaluation of the ICG-sOSu-panitumumab revealed excellent target-specific uptake with minimal liver uptake in athymic nude mice bearing HER1-positive s.c. LS-174T xenografts.

One of the important confirmatory findings in this study was that despite the use of the improved aqueous solubility properties of ICG-sOSu, the formation of HMW aggregates of panitumumab during the conjugation reaction occurred. This conclusion was supported by the strong absorbance at 280 nm, and the staining pattern (>150 kDa) shown on the colloidal blue-stained SDS and native gels in the collected samples of aggregates. Because the HMW aggregates are composed of mAb, the yields of the desired products were affected. For example, the yield of the desired ICG-sOSu-panitumumab product in the 20× ICG-sOSu dye reaction was ∼19%, and

dx.doi.org/10.1021/bc500312w | *Bioconjugate Chem.* 2014, 25, 1801−1810

significant amounts of the mAb were consumed in the creation of the HMW aggregates as seen from the large peak at RT = 12.5 min (Figure 1). In contrast, the product yield was much higher (~72%) from the 5× ICG-sOSu dye reaction with a smaller amount of the HMW entity being generated. However, the higher yield with the lower ICG-sOSu:mAb molar reaction ratio then is at the cost of the number of ICG-sOSu molecules conjugated to the antibody. Thus, one should exercise caution in optimization of the ICG-related conjugation reactions.

All three purified ICG-sOSu-panitumumab conjugates (**1**, **2**, and **3**) exhibited two absorbance peaks at 720 and 800 nm. Both of the absorption maxima were red-shifted as compared with 715 and 780 nm for ICG-sOSu, which is in agreement with previous publications where dye was bound to a large molecule.[15] In addition, as was observed from the absorption spectra data of the study described herein, the intensity ratio between the two absorbance peaks, 720 nm relative to 800 nm, increased with increasing equivalents of ICG-sOSu (Figure 2A). This might be caused by the increased number of ICG-sOSu conjugated to panitumumab (~1, 2, and 5 for **1**, **2**, and **3**, respectively). Similar phenomenon was observed in previous studies.[16,23] With the increasing ICG concentration in aqueous solution, the absorption peak shifts from 780 nm to the wavelength of 695 nm as a result of aggregation of ICG molecules from monomer to oligomer.[16]

Dialysis or PD-10 filtration has been commonly performed after conjugation to remove excess dye.[24] While convenient, unfortunately, neither is well suited for removing aggregates larger than 150 kDa, nor effective at removing noncovalently bound ICG-sOSu. After purification by SE-HPLC and subsequent ethyl acetate extraction, a pure covalently linked conjugation product was obtained. The advantage of using purified and thus validated ICG-sOSu conjugation products is multifold. First, elimination of the noncovalently bound dye reduces nonspecific liver retention and thus allows for high fidelity imaging of the targeted organs. As observed from our previous studies, the uptake in tumor is the highest at day 3 postinjection of the radiolabeled panitumumab (Y-86 or Zr-89), while all other organs have low uptake in the same animal model.[19,20] Differently, the fluorescence intensity in liver was also observed in this study, in addition to tumor, using the SE-HPLC purified conjugation products. Actually, high liver uptake has been observed in previous studies with ICG-sOSu conjugates,[25,26] which might be directly related to the presence of aggregate products and/or noncovalently bound ICG-sOSu. The liver retention was greatly diminished with the doubly purified conjugation product. These findings could open a new avenue for the development of targeted imaging agents for liver disease using ICG-sOSu conjugates and quite possibly other structurally related NIR dyes useful for noninvasive optical imaging. The second advantage is that this methodology is more accurate for determining the number of dye molecules conjugated to a mAb in an actual covalently linked conjugate and thus translates forward as an agent suitable for monitoring antigen (e.g., HER1) expression in tumor. For example, the calculated number of ICG-sOSu conjugated to mAb was ~2 after SE-HPLC purification (product **2**). After elimination of the noncovalently bound ICG-sOSu, the number of ICG-sOSu conjugated to mAb dropped to ~1.2 for product **5**. In addition, false positive results, due to noncovalently bound ICG-sOSu, could be generated for antigen expression since part of the released ICG-sOSu might localize in tumor due to its leaky vasculature or be released from the mAb postinternalization in the lysozomal compartment. Lastly, pure products are favorable for clinical application and Food and Drug Administration (FDA) approval. PEGylation of bioconjugates has been reported to prevent aggregation of ICG-sOSu in aqueous solution,[18] as well as to reduce immunogenicity and improve imaging performance.[27] The synthesis and characterization of PEGylated ICG-sOSu conjugation products are currently being pursued for future studies to increase product yields as well as for the reasons just cited.

There were some limits on instrumentation in this study. The UV detector used for the SE-HPLC was limited in wavelengths to 280 nm, which is not optimal for detection the ICG-sOSu. Detection of ICG-sOSu would better be performed at longer wavelengths, e.g., 700−800 nm. Therefore, the in-line analysis of the SE-HPLC with our UV detector might not be the most accurate for the multicomponent mixture. However, this did not pose a significant obstacle since collection of the individual peaks and analysis by a spectrophotometer provided confirmatory information on the samples from the SE-HPLC. For example, a peak was observed at 27.2 min, which was the same RT of free ICG-sOSu, yet this was demonstrated to be impurities from the starting material (purity of the commercial ICG-sOSu was ~80%; see Supporting Information Figure S1) since there was no absorbance at 700−800 nm seen in the spectrophotometer profile for this peak.

In conclusion, ICG-sOSu-panitumumab conjugation products in this study were purified and characterized for their optical, chemical, and biological properties. Double purification was performed first by SE-HPLC to remove the HMW aggregates and LMW impurities, and second by ethyl acetate extraction to abrogate noncovalently bound ICG-sOSu. The validated ICG-sOSu-panitumumab was successfully applied in tumor localization with minimal liver uptake in athymic nude mice bearing HER1-positive LS-174T tumor xenografts. Further studies will, however, be necessary to explore the new strategies of reducing the formation of HMW aggregates and better define the potential applications in the clinical settings. The covalently linked conjugation products herein provide promise in the development of clinically viable and reproducible dye-conjugated mAb for optical imaging applications.

EXPERIMENTAL PROCEDURES

Materials. ICG-*N*-hydroxysulfosuccinimide ester (ICG-sulfo-OSu, 2-[7-[1,3-Dihydro-1,1-dimethyl-3-(4-sulfobutyl)-2*H*-benzo[e]indol-2-ylidene]-1,3,5-heptatrienyl]-1,1-dimethyl-3-[5-(3-sulfosuccinimidyl)oxycarbonylpentyl]-1*H*-benzo[e]-indolium) was purchased from AAT Bioquest (Sunnyvale, CA). Panitumumab (Amgen, Thousand Oaks, CA) was obtained from the NIH Veterinary Resources Pharmacy. HuM195, an anti-CD33 mAb, was generously provided by Dr. McDevitt from Memorial Sloan Kettering Cancer Center.

Antibody Conjugation. The amine-reactive dye ICG-sOSu was first dissolved in anhydrous DMSO (Sigma-Aldrich, Saint Louis, MO). Solutions of panitumumab (5 mg, 33 nmol) were incubated with ICG-sOSu at molar ratios of ICG-sOSu:mAb of 5, 10, and 20 (5×, 10×, and 20×) in conjugation buffer (0.002 M $NaHCO_3$ + 0.048 M Na_2CO_3 + 0.15 M NaCl, pH 8.5) for 1 h in the dark at 37 °C with gentle mixing at 750 rpm. Total volume (250 μL) and DMSO percentage (16%) were constant for all reactions. After incubation, the three reaction solutions were analyzed, respectively, with the same loading volume by SE-HPLC on a Beckman System Gold HPLC (1

dx.doi.org/10.1021/bc500312w | *Bioconjugate Chem.* 2014, 25, 1801−1810

mL/min flow rate) fitted with a tandem-column of a TSK gel G3000SW linked to a TSK gel G4000SW (TOSOH Bioscience, LLC) using phosphate buffer (67 mM $NaPO_4$ + 100 mM KCl, pH 6.8) as eluent. And then, each solution was purified by SE-HPLC at the same condition. The % conjugation products in the reaction solution is defined as derived from the SE-HPLC profile using Beckman Coulter's 32 Karat software and is equal to the peak area for the desired products/total area of all peaks ×100. "All peaks" include that for HMW entities, desired products, as well as free dye. Similar procedures were applied to conjugate ICG-sOSu to the negative control mAb, HuM195, at a 10:1 reaction molar ratio. Identical conditions and columns were used for purification of the ICG-sOSu-HuM195 conjugated product. MW standards (Bio-Rad Laboratories, Hercules, CA) were used to calibrate the HPLC methods. Absorbance spectra were recorded using an Agilent 8453 spectrophotometer (Santa Clara, CA) for the isolated products.

Calculation. The amount of dye conjugated to panitumumab was calculated as previously described.[24] Calculations were performed based on the following equation:

$$\text{amount of dye conjugated to panitumumab} = \frac{A_{\text{Dye}}/\varepsilon^{\text{M}}{}_{\text{Dye}}}{(A_{280} - A_{\text{Dye}} \times \text{CF})/\varepsilon^{\text{M}}{}_{A280}}$$

where A_{Dye} = absorbance of ICG-sOSu at the peak wavelength; $\varepsilon^{\text{M}}{}_{\text{Dye}}$ = the molar extinction coefficient of ICG-sOSu at the same wavelength as A_{Dye}; $\varepsilon^{\text{M}}{}_{280}$ = the molar extinction coefficient of panitumumab at 280 nm; CF (correction factor) = $A_{280\text{-dye}}/A_{\text{Dye}}$. Accordingly, the % yield of the conjugation product is calculated that is equal to the obtained moles of conjugation products/total moles of panitumumab in the reaction ×100.

Competition Assay. The immunoreactivity of the conjugation products was evaluated based on a previously published competition radioimmunoassay.[18] Briefly, serial dilutions of the test solutions were performed to allow 0.02–1000 ng of each sample to be added in triplicate to wells of 96-well plates coated with 50 ng human epidermal growth factor receptor (hEGFR). ^{125}I-panitumumab[18] (~50 000 cpm) was then added and incubated for 4 h at 37 °C. After washing the wells three times with PBS containing 1% bovine serum albumin (BSA), 0.2 M NaOH was added to mobilize the bound radioactivity followed by collection of the activity using cotton filters. Activity was measured in a 1480 WIZARD 3″ automatic γ-counter (PerkinElmer, Shelton, CT). Results were plotted as percent inhibition vs concentration of the samples. The purified ICG-sOSu-HuM195 conjugated product served as a negative control.

***In Vivo* and *Ex Vivo* Optical Imaging.** Animal studies were performed in female athymic (nu/nu) mice (Charles River Laboratories, Wilmington, MA). All animal protocols were approved by the National Cancer Institute Animal Care and Use Committee. HER-1 positive human colorectal carcinoma LS-174T cells (American Type Culture Collection (ATCC)) were cultured in Dulbecco's Modified Eagle's Medium (DMEM) containing 10% FetalPLEX (Gemini Bio-Products, West Sacramento, CA) and 10 mM glutamine. Mice were injected subcutaneously in the right shoulder with 1×10^6 LS-174T cells in 200 μL saline. When tumors were ~400 mm^3, mice (n = 5) were injected intravenously with **1** or **2** at indicated doses, or ICG-sOSu-HuM195 (negative control, 20 μg). Optical imaging was performed on days 1, 2, 3, and 7 postinjection of the ICG-sOSu-panitumumab using a Maestro *in vivo* Fluorescence Imaging System equipped with the following filters: excitation wavelength 700 to 770 nm, emission wavelength 790 nm (Cambridge Research & Instrumentation, Woburn, MA). Ketamine/Xylazine (100/10 mg/kg, respectively) was used to anesthetize animals throughout the imaging process. For blocking studies, excess panitumumab (1 mg) was injected to block the receptor sites 1 h prior to injection of the ICG-sOSu-panitumumab. For quantitative analysis, regions of interest (ROI) were drawn over tumors and thigh muscles (as background). The average fluorescence signal of each ROI was measured and recorded. Results were expressed as tumor-to-background ratio. To evaluate the biodistribution of the conjugation products in mice, organs (heart, lung, liver, spleen, kidney, intestine, tumor) were harvested from mice at day 3 postinjection of agents (n = 3) and imaged. Imaging was repeated as described above to evaluate the qualities of the ethyl acetate extracted ICG-sOSu-panitumumab conjugate.

Polyacrylamide Gel Electrophoresis. SDS polyacrylamide gel electrophoresis (SDS-PAGE) was performed as previously described.[18] Briefly, samples (2 μg), with or without β-mercaptoethanol, were loaded into each lane of 4–20% precast tris-glycine polyacrylamide gels (Invitrogen, Carlsbad, CA). Panitumumab (2 μg) served as a reference material and resolved at 120 V. Protein was visualized by colloidal blue staining; NIR light was captured by the Maestro Fluorescence Imaging System. Samples were also analyzed by nondenaturing (native) electrophoresis to further investigate the interaction of ICG-sOSu and panitumumab in the conjugation products. Native sample buffer and native running buffer were used for nondenaturing electrophoresis.

Chemical Purification of Covalently Conjugated Products. Extraction of HPLC-purified ICG-sOSu-panitumumab was performed using conditions described elsewhere.[22] In brief, products were subjected to ethyl acetate extraction (1:1) by vigorous shaking for 30 min. The separated aqueous layer was then immediately treated to buffer exchange in PBS using a Centriprep centrifugal filter device (Millipore, Bedford, MA) to remove trace residual ethyl acetate. The number of ICG-sOSu conjugated to panitumumab was calculated again as described above. This new number was used to revise the number obtained from just SE-HPLC purification to get the percentage of covalently bound dye in the SE-HPLC purified products.

Statistical Analysis. Quantitative data are expressed as the mean plus/minus standard error of mean (SEM). One-way ANOVA was used to determine the statistical significance for the tumor-to-background or tumor-to-organ ratio in different treatment groups. Significant difference was considered when $p < 0.05$.

■ ASSOCIATED CONTENT

Supporting Information

RP-HPLC profile of ICG-sulfo-OSu (Figure S1); SE-HPLC data of ICG-sOSu-HuM195 (Figure S2); *in vitro* fluorescence microscopy images (Figure S3); *ex vivo* NIR fluorescence image of the dissected organs from athymic mice bearing HER1-positive peritoneal LS-174T tumor xenografts (Figure S4); SE-HPLC profile of the doubly purified ICG-sOSu-panitumumab (**5**) (Figure S5). This material is available free of charge via the Internet at http://pubs.acs.org.

AUTHOR INFORMATION

Corresponding Author

*Phone: 301-496-0591. Fax: 301-402-1923. E-mail: martinwb@mail.nih.gov.

Notes

The authors declare no competing financial interest.

ACKNOWLEDGMENTS

This research was supported by the Intramural Research Program of the NIH, National Cancer Institute, Center for Cancer Research. We would like to thank the EIB Microscopy and Digital Imaging Facility and Dr. Michael Kruhlak for the technical assistance in fluorescence microscopy.

ABBREVIATIONS

NIRF, near-infrared fluorescence; mAb, monoclonal antibody; SE-HPLC, size-exclusion high-performance liquid chromatography; PEG, polyethylene glycol; HMW, high molecular weight; LMW, low molecular weight; ICG-sOSu, ICG-sulfo-OSu, ICG-*N*-hydroxysulfosuccinimide ester; RT, retention time; SDS-PAGE, sodium dodecyl sulfate polyacrylamide gel electrophoresis

REFERENCES

(1) van Dam, G. M., Themelis, G., Crane, L. M., Harlaar, N. J., Pleijhuis, R. G., Kelder, W., Sarantopoulos, A., de Jong, J. S., Arts, H. J., van der Zee, A. G., Bart, J., Low, P. S., and Ntziachristos, V. (2011) Intraoperative tumor-specific fluorescence imaging in ovarian cancer by folate receptor-α targeting: first in-human results. *Nat. Med. 17*, 1315−1319.

(2) Metildi, C. A., Kaushal, S., Hardamon, C. R., Snyder, C. S., Pu, M., Messer, K. S., Talamini, M. A., Hoffman, R. M., and Bouvet, M. (2012) Fluorescence-guided surgery allows for more complete resection of pancreatic cancer, resulting in longer disease-free survival compared with standard surgery in orthotopic mouse models. *Journal of the American College of Surgeons 215*, 126−135.

(3) Tanaka, E., Choi, H. S., Fujii, H., Bawendi, M. G., and Frangioni, J. V. (2006) Image-guided oncologic surgery using invisible light: completed pre-clinical development for sentinel lymph node mapping. *Ann. Surg. Oncol. 13*, 1671−1681.

(4) Luker, G. D., and Luker, K. E. (2008) Optical imaging: current applications and future directions. *J. Nucl. Med. 49*, 1−4.

(5) Kim, S., Lim, Y. T., Soltesz, E. G., De Grand, A. M., Lee, J., Nakayama, A., Parker, J. A., Mihaljevic, T., Laurence, R. G., Dor, D. M., Cohn, L. H., Bawendi, M. G., and Frangioni, J. V. (2004) Near-infrared fluorescent type II quantum dots for sentinel lymph node mapping. *Nat. Biotechnol. 22*, 93−97.

(6) Soltesz, E. G., Kim, S., Laurence, R. G., DeGrand, A. M., Parungo, C. P., Dor, D. M., Cohn, L. H., Bawendi, M. G., Frangioni, J. V., and Mihaljevic, T. (2005) Intraoperative sentinel lymph node mapping of the lung using near-infrared fluorescent quantum dots. *The Annals of Thoracic Surgery 79*, 269−277.

(7) Alander, J. T., Kaartinen, I., Laakso, A., Pätilä, T., Spillmann, T., Tuchin, V. V., Venermo, M., and Välisuo, P. (2012) A review of indocyanine green fluorescent imaging in surgery. *Int. J. Biomed. Imaging. 2012*, 940585.

(8) Ishizawa, T., Fukushima, N., Shibahara, J., Masuda, K., Tamura, S., Aoki, T., Hasegawa, K., Beck, Y., Fukayama, M., and Kokudo, N. (2009) Real-time identification of liver cancers by using indocyanine green fluorescent imaging. *Cancer 115*, 2491−2504.

(9) Morita, Y., Sakaguchi, T., Unno, N., Shibasaki, Y., Suzuki, A., Fukumoto, K., Inaba, K., Baba, S., Takehara, Y., Suzuki, S., and Konno, H. (2013) Detection of hepatocellular carcinomas with near-infrared fluorescence imaging using indocyanine green: its usefulness and limitation. *Int. J. Clin. Oncol. 18*, 232−241.

(10) Nakajima, T., Mitsunaga, M., Bander, N. H., Heston, W. D., Choyke, P. L., and Kobayashi, H. (2011) Targeted, activatable, in vivo fluorescence imaging of prostate-specific membrane antigen (PSMA) positive tumors using the quenched humanized J591 antibody-indocyanine green (ICG) conjugate. *Bioconjugate Chem. 22*, 1700−1705.

(11) Yano, H., Muguruma, N., Ito, S., Aoyagi, E., Kimura, T., Imoto, Y., Cao, J., Inoue, S., Sano, S., Nagao, Y., and Kido, H. (2006) Fab fragment labeled with ICG-derivative for detecting digestive tract cancer. *Photodiagn. Photodyn. Ther. 3*, 177−183.

(12) Bando, T., Muguruma, N., Ito, S., Musashi, Y., Inayama, K., Kusaka, Y., Tadatsu, M., Kunio, I., Irimura, T., Shibamura, S., and Takesako, K. (2002) Basic studies on a labeled anti-mucin antibody detectable by infrared-fluorescence endoscopy. *J. Gastroenterol. 37*, 260−269.

(13) Ito, S., Muguruma, N., Kakehashi, Y., Hayashi, S., Okamura, S., Shibata, H., Okahisa, T., Kanamori, M., Shibamura, S., Takesako, K., Nozawa, M., Ishida, K., and Shiga, M. (1995) Development of fluorescence-emitting antibody labeling substance by near-infrared ray excitation. *Bioorg. Med. Chem. Lett. 5*, 2689−2694.

(14) Withrow, K. P., Gleysteen, J. P., Safavy, A., Skipper, J., Desmond, R. A., Zinn, K., and Rosenthal, E. L. (2007) Assessment of indocyanine green-labeled cetuximab to detect xenografted head and neck cancer cell lines. *Otolaryngol. Head Neck Surg. 137*, 729−734.

(15) Zheng, X., Xing, D., Zhou, F., Wu, B., and Chen, W. R. (2011) Indocyanine green-containing nanostructure as near infrared dual-functional targeting probes for optical imaging and photothermal therapy. *Mol. Pharmaceutics 8*, 447−456.

(16) Landsman, M. L., Kwant, G., Mook, G. A., and Zijlstra, W. G. (1976) Light-absorbing properties, stability, and spectral stabilization of indocyanine green. *J. Appl. Physiol. 40*, 575−583.

(17) Urbanska, K., Romanowska-Dixon, B., Matuszak, Z., Oszajca, J., Nowak-Sliwinska, P., and Stochel, G. (2002) Indocyanine green as a prospective sensitizer for photodynamic therapy of melanomas. *Acta Biochim. Polym. 49*, 387−391.

(18) Villaraza, A. J., Milenic, D. E., and Brechbiel, M. W. (2010) Improved speciation characteristics of PEGylated indocyanine green-labeled Panitumumab: revisiting the solution and spectroscopic properties of a near-infrared emitting anti-HER1 antibody for optical imaging of cancer. *Bioconjugate Chem. 21*, 2305−2312.

(19) Nayak, T. K., Garmestani, K., Baidoo, K. E., Milenic, D. E., and Brechbiel, M. W. (2010) Preparation, biological evaluation, and pharmacokinetics of the human anti-HER1 monoclonal antibody panitumumab labeled with ^{86}Y for quantitative PET of carcinoma. *J. Nucl. Med. 51*, 942−950.

(20) Nayak, T. K., Garmestani, K., Milenic, D. E., and Brechbiel, M. W. (2012) PET and MRI of metastatic peritoneal and pulmonary colorectal cancer in mice with human epidermal growth factor receptor 1-targeted ^{89}Zr-labeled panitumumab. *J. Nucl. Med. 53*, 113−120.

(21) Bunschoten, A., Buckle, T., Kuil, J., Luker, G. D., Luker, K. E., Nieweg, O. E., and van Leeuwen, F. W. (2012) Targeted non-covalent self-assembled nanoparticles based on human serum albumin. *Biomaterials 33*, 867−875.

(22) Hirata, T., Kogiso, H., Morimoto, K., Miyamoto, S., Taue, H., Sano, S., Muguruma, N., Ito, S., and Nagao, Y. (1998) Synthesis and reactivities of 3-indocyanine-green-acyl-1,3-thiazolidine-2-thione (ICG-ATT) as a new near-infrared fluorescent-labeling reagent. *Bioorg. Med. Chem. 6*, 2179−2184.

(23) Yuan, B., Chen, N., and Zhu, Q. (2004) Emission and absorption properties of indocyanine green in Intralipid solution. *J. Biomed. Opt. 9*, 497−503.

(24) Haugland, R. P. (2000) Antibody conjugates for cell biology. *Curr. Protoc. Stem Cell Biol.*, 16.5.1−16.5.22.

(25) Xu, Y., Zanganeh, S., Mohammad, I., Aguirre, A., Wang, T., Yang, Y., Kuhn, L., Smith, M. B., and Zhu, Q. (2013) Targeting tumor hypoxia with 2-nitroimidazole-indocyanine green dye conjugates. *J. Biomed. Opt. 18*, 66009.

(26) Sano, K., Nakajima, T., Miyazaki, K., Ohuchi, Y., Ikegami, T., Choyke, P. L., and Kobayashi, H. (2013) Short PEG-linkers improve the performance of targeted, activatable monoclonal antibody-indocyanine green optical imaging probes. *Bioconjugate Chem. 24*, 811−816.
(27) Chapman, A. P. (2002) PEGylated antibodies and antibody fragments for improved therapy: a review. *Adv. Drug Delivery Rev. 54*, 531−545.